Journal of
Civil Engineering and Structures

Journal homepage: www.journalces.com

Original paper

Effect of storey number on Vierendeel mechanism in progressive collapse of RC frame structures

Peyman Beiranvand [1*], Farzad Lari [2], Majid Alipour [3] and Mosayeb Maleki [4]
[1] School of Civil Engineering, Iran University of Science and Technology (IUST), Narmak, Tehran, Iran.
[2] Department of Civil Engineering, Islamic Azad University, South Tehran Branch, Tehran, Iran.
[3,4] Department of Civil Engineering, Islamic Azad University, Khorramabad Branch, Khorramabad, Iran.

ARTICLE INFO

Article history:
Received 19 September 2025
Accepted 7 March 2026

Keywords:

RC frame structures
Column removal scenario
Load redistribution mechanisms
Multi-storey buildings
Numerical simulation
LS-DYNA

ABSTRACT

Progressive collapse of reinforced concrete (RC) structures can lead to severe casualties and extensive property damage. Hence, reliable evaluation of structural resistance against such collapse is essential. This study numerically examines how the number of storeys influences the activation and contribution of the Vierendeel mechanism in RC frames subjected to corner column removal. For this purpose, finite element models of multi-storey RC frames were developed using LS-DYNA and validated against experimental tests conducted by the authors. The validated models were then used to analysis frames ranging from one to six storeys. The results show that in multi-storey substructures, additional plastic hinges form at beam ends adjacent to the removed column in upper storeys (second to top), as well as at the lower end of the corner column in the first storey. Compared to the single-storey substructure (where no Vierendeel mechanism develops), the average ultimate resistance per storey in multi-storey cases increased by 14.1% to 18.3%. However, the contribution of the Vierendeel mechanism to the overall ultimate resistance slightly decreased as the number of stores increased.

DOI: https://doi.org/10.21859/jces.10179

1. Introduction

The unexpected failure of a single structural component can trigger a chain reaction that leads to the collapse of an entire building or a disproportionately large portion of it a phenomenon commonly referred to as progressive collapse. Such events have repeatedly resulted in catastrophic consequences, including extensive loss of life and severe economic damage. In response, many nations have revised their building codes and design guidelines to enhance structural robustness against this type of failure (U.S. General Services Administration, 2003; Department of Defense, 2009; European Committee for Standardization, 2006; Ministry of Housing and Urban-Rural Development of China, 2010a, 2010b). Among the various assessment methods, the alternate load path (ALP) approach has gained wide acceptance because it evaluates the capacity of the remaining structure to bridge over a removed load-bearing member without relying on the failed element.

To simplify the analysis of multi-storey buildings under progressive collapse, earlier research often focused on single-storey beam–slab or beam–column substructures. Under a corner column removal scenario, these substructures were found to primarily develop cantilever flexural mechanisms (Qian & Li, 2012a, 2012b; Lim et al., 2017; Du et al., 2020; Xu et al., 2021; Qin et al., 2022). However, these studies largely overlooked the contribution of the upper storeys, which can provide additional resistance through what is known as Vierendeel mechanism (VM) a frame action that transfers loads via bending and shear in the members without relying on diagonal bracing.

Evidence of VM has been observed in both experimental and numerical investigations of multi-storey reinforced concrete (RC) frames. For instance, Sasani et al. (2007, 2008, 2011) and Adam et al. (2020) and Buitrago et al. (2023) demonstrated that VM plays a dominant role in redistributing loads after the loss of corner columns in full-scale structures. More recently, numerical studies have further clarified the collapse mechanisms of multi-storey systems. Qiao et al. (2018, 2020)

[*]Corresponding author Email: p_beiranvand@civileng.iust.ac.ir

Please cite this article as: Beiranvand, P., Lari, F., Alipour, M., and Maleki, M. (2026). Effect of storey number on Vierendeel mechanism in progressive collapse of RC frame structures. *Journal of Civil Engineering and Structures*, 10(1), pp. 17-23.

developed analytical models that combine flexural action and VM for steel frames, while Li et al. (2016) showed that the presence of VM induces different internal force distributions in beams across various storeys of an eight-storey RC frame. Qian et al. (2021) compared single- and multi-storey substructures and noted that VM is particularly effective in the bottom storey.

Despite these advances, there remains a lack of systematic understanding of how the number of storeys influences the development and quantitative contribution of VM in progressive collapse resistance, especially under corner column loss. To address this gap, the present study numerically examines single-storey and multi-storey RC substructures ranging from one to six storeys. Finite element models are developed using LS-DYNA and validated against experimental data from the authors' own tests. The validated models are then used to analyse the evolution of plastic hinges and load–displacement responses, with particular attention to the role of storey number in the activation and efficiency of VM.

2. Materials and Methods

2.1. Experimental investigation

To provide a reliable basis for calibrating the numerical models, the authors carried out quasi-static loading tests on two reduced-scale RC substructures. These specimens were extracted from a six-storey prototype building, which had been designed in compliance with the relevant Chinese design provisions (Ministry of Housing and Urban-Rural Development of China, 2010a, 2010b). The prototype structure, depicted in Fig. 1, featured a regular plan with storey heights and bay widths typical of residential construction. The specified dead and live floor loads were 6.17 kN/m² and 2.0 kN/m², respectively, with an additional line load of 5.24 kN/m applied to the perimeter beams. It is worth noting that the reinforcement arrangements in the third through fifth storeys were identical, which facilitated the extraction of consistent substructure specimens.

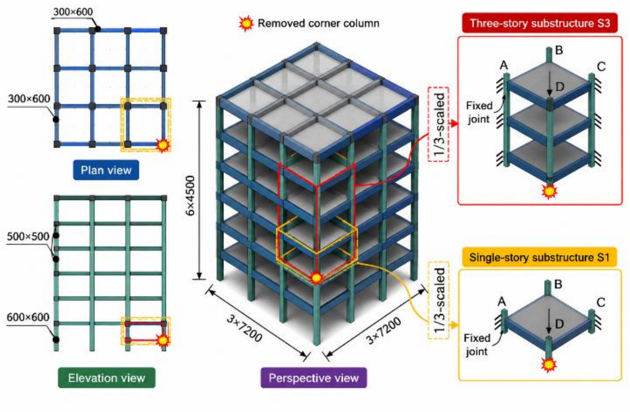

Fig 1. Geometric layout and reinforcement details of the six-storey prototype RC frame (dimensions in mm).

The first specimen, designated S1, represented a single-storey subassembly taken from the corner region of the third floor. The second specimen, labelled S3, was a three-storey subassembly spanning the third to fifth floors, thereby capturing the continuity of vertical load-carrying elements over multiple levels. Fig. 2 provides detailed illustrations of the reinforcement layouts and cross-sectional dimensions for both specimens. The concrete cover thicknesses were set at 10 mm for slabs, 15 mm for beams, and 20 mm for columns, reflecting standard detailing practice.

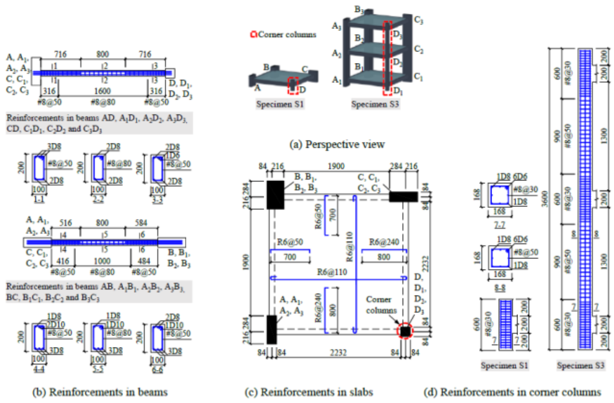

Fig 2. Reinforcement configuration and cross-sectional dimensions of test specimens S1 and S3 (dimensions in mm).

The experimental setup is shown schematically in Fig. 3. A displacement-controlled hydraulic actuator was employed to impose monotonically increasing vertical displacement on the top of the corner column, simulating the sudden loss of support at that location. To ensure that only vertical forces were transmitted, the loading system incorporated one-way pin connections that allowed free rotation of the column end, thereby preventing the introduction of unintended horizontal forces or bending moments. The measured cylinder compressive strength of the concrete was 21.8 MPa, and the key tensile properties of the steel reinforcement are summarized in Table 1.

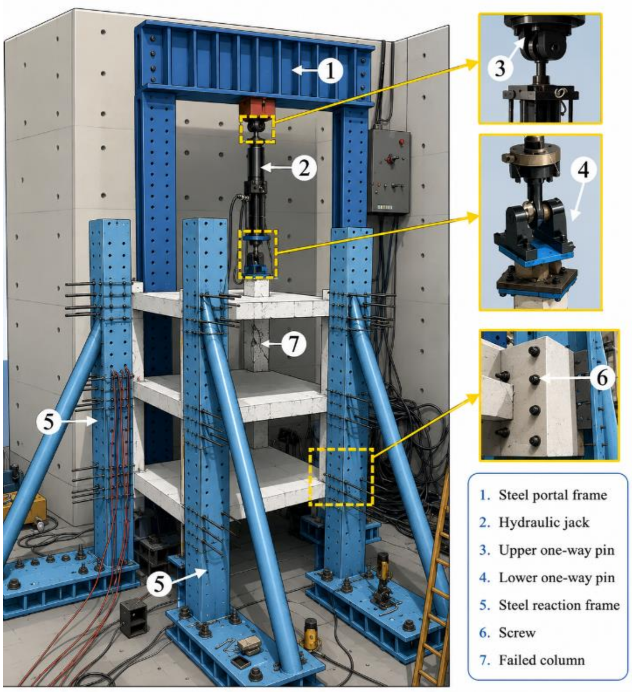

Fig 3. Schematic view of the quasi-static test setup used for the experimental program.

Please cite this article as: Beiranvand, P., Lari, F., Alipour, M., and Maleki, M. (2026). Effect of storey number on Vierendeel mechanism in progressive collapse of RC frame structures. *Journal of Civil Engineering and Structures*, 10(1), pp. 17-23.

Table 1. Mechanical properties of the reinforcing steel bars used in the experimental program.

Reinforcement type	Bar designation	Nominal diameter (mm)	Modulus of elasticity (GPa)	Yield stress (MPa)	Tensile strength (MPa)	Failure strain (%)
Galvanized tie wire	#8	3.8	82	342	382	28.0
Plain mild steel	R6	5.6	189	379	712	24.5
Plain mild steel	D6	6.0	172	343	629	96.1
Deformed high-yield	D8	7.4	196	393	684	49.6
Deformed high-yield	D10	10.0	192	487	587	16.4

2.2. Development of the Finite Element Models

The numerical simulations were performed using the explicit finite element code LS-DYNA (Livermore Software Technology Corporation, 2016). A systematic approach was adopted to define material behaviour, element formulations, interface connections, boundary conditions, and mesh refinement, as detailed in the following subsections.

2.2.1. Material models and element types

For the concrete components, the Continuous Surface Cap Model (CSCM), implemented as *MAT_159 in LS-DYNA, was selected. This model is particularly suitable for simulating quasi-brittle materials because it captures key features such as strain-softening, shear dilation, pressure-dependent yielding, and strain-rate sensitivity. Although the model offers an automatic parameter-generation option for normal-strength concrete, the present study adopted the user-defined input route. This approach, while requiring approximately 50 input variables derived from the uniaxial compressive strength and maximum aggregate size, has been shown to reduce the overestimation of structural stiffness when the elastic modulus and fracture energy are appropriately scaled down (Murray, 2007; Yu et al., 2018). Consequently, this more detailed calibration was employed to enhance the fidelity of the numerical predictions.

The steel reinforcement bars and the loading plates were modelled using an elastic-perfectly plastic material law (*MAT_003), with the elastic modulus, yield stress, and ultimate strain taken directly from the material test results. For the spatial discretization, the concrete and steel plates were represented by eight-node hexahedral solid elements with reduced integration to minimize shear locking. The reinforcing bars were discretized using two-node Hughes-Liu beam elements, which incorporate 2×2 Gauss quadrature for accurate flexural response.

2.2.2. Connection modelling, boundary constraints, and loading protocol

The continuity between beams, columns, slabs, and steel bearing plates was ensured by Boolean operations during geometry construction, thereby creating a monolithic connection at all interfaces. The bond between steel rebars and the surrounding concrete was assumed to be perfect, as the development lengths provided in the prototype design were sufficient to prevent anchorage failure a condition confirmed by the absence of bond-slip damage in the physical tests. This perfect-bond assumption was implemented using the CONSTRAINED_LAGRANGE_IN_SOLID keyword. The confinement effect of transverse stirrups on the longitudinal bars was represented through automatic single-surface contact (CONTACT_AUTOMATIC_SINGLE_SURFACE).

Fixed support conditions were prescribed at the steel plates attached to the outer faces of the columns that remained intact. The analysis proceeded in two sequential steps: first, the self-weight and permanent floor loads were applied to the entire model; second, a monotonically increasing vertical displacement was imposed on the plate fixed to the top of the corner column to simulate the progressive downward movement following column loss.

2.2.3. Mesh size

A sensitivity analysis was conducted on Specimen S1 to determine an optimal balance between computational expense and solution accuracy. Three mesh densities were examined, with solid element sizes of 50 mm, 25 mm, and 15 mm, paired with beam element sizes of 100 mm, 50 mm, and 30 mm, respectively. The corresponding simulation run-times were 3, 10, and 47 hours, while the predicted ultimate resistances were 17.9 kN, 20.1 kN, and 21.1 kN Given that the 25 mm/50 mm mesh provided a satisfactory compromise capturing the key structural response with acceptable computational effort this configuration was adopted for all subsequent analyses. Fig. 4 presents a visualization of the final finite element mesh for Specimen S1 as a representative example.

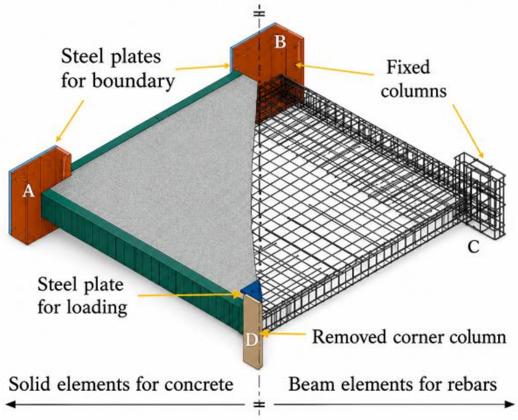

Fig 4. Three-dimensional finite element mesh representation of Specimen S1 (illustrative example).

2.3. Verification of the numerical approach

The validity of the proposed FE modelling strategy was assessed by comparing the numerical predictions against the experimental measurements for both Specimens S1 and S3. Fig. 5 presents the superimposed load vertical displacement traces, showing good correlation in terms of both ascending and descending branches. The numerical ultimate loads were determined as 20.1 kN and 72.0 kN for S1 and S3, respectively, which deviated from the test results by 0 % and 7.9 % well within acceptable engineering tolerances.

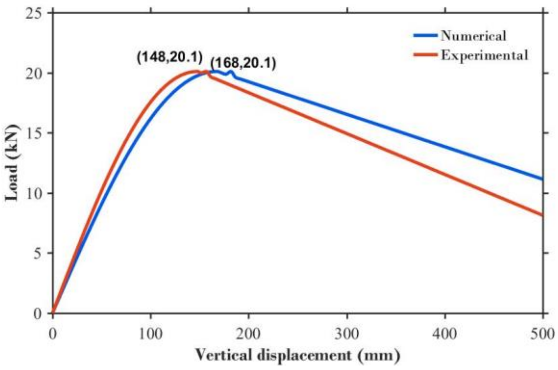

(a)

Please cite this article as: Beiranvand, P., Lari, F., Alipour, M., and Maleki, M. (2026). Effect of storey number on Vierendeel mechanism in progressive collapse of RC frame structures. *Journal of Civil Engineering and Structures*, 10(1), pp. 17-23.

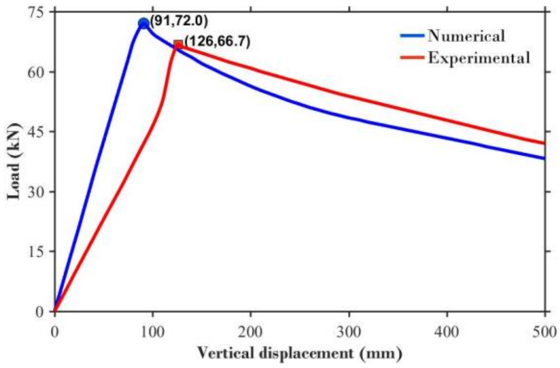

(b)

Fig 5. Comparison of numerically predicted and experimentally measured load versus vertical displacement responses for (a) Specimen S1 and (b) Specimen S3.

Furthermore, the spatial distribution of plastic hinges was compared, as illustrated in Fig. 6. Owing to symmetry, only the facade containing side beam CD is shown. In the numerical models, plastic hinge formation was identified through combined indicators of rebar yielding and effective plastic strain localization in the concrete. The locations of these hinges matched those observed in the experiments with remarkable consistency. These favorable comparisons confirm that the developed FE models are sufficiently accurate to serve as a reliable platform for the parametric study examining the influence of storey number on Vierendeel mechanism, which is presented in the subsequent sections.

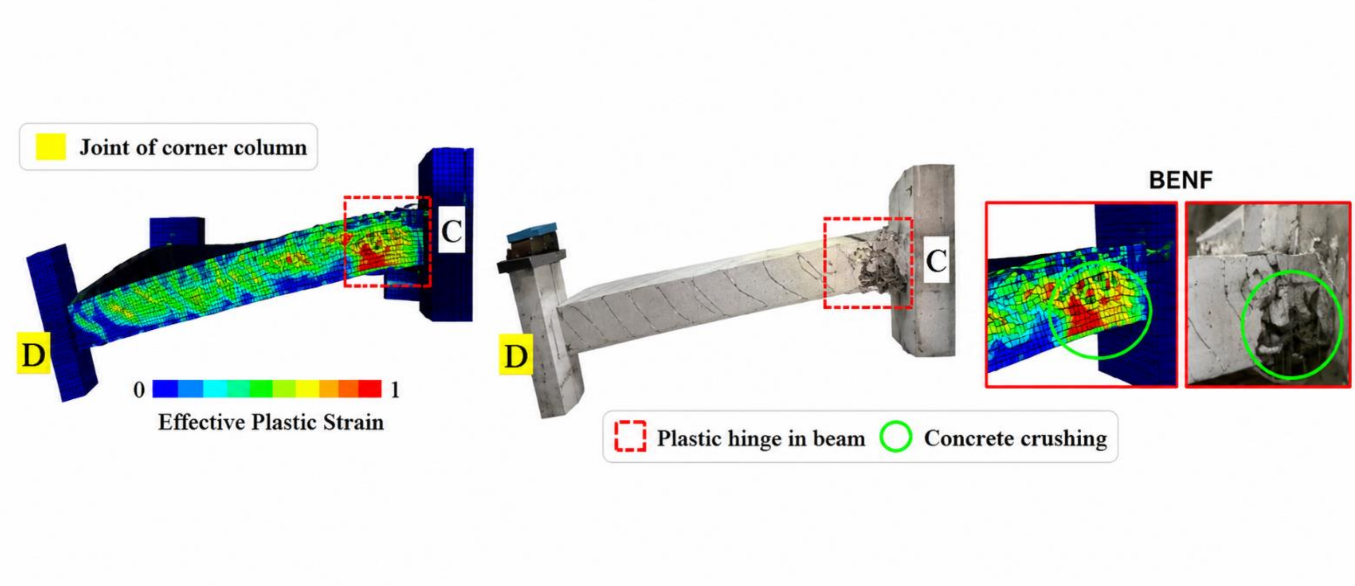

(a)

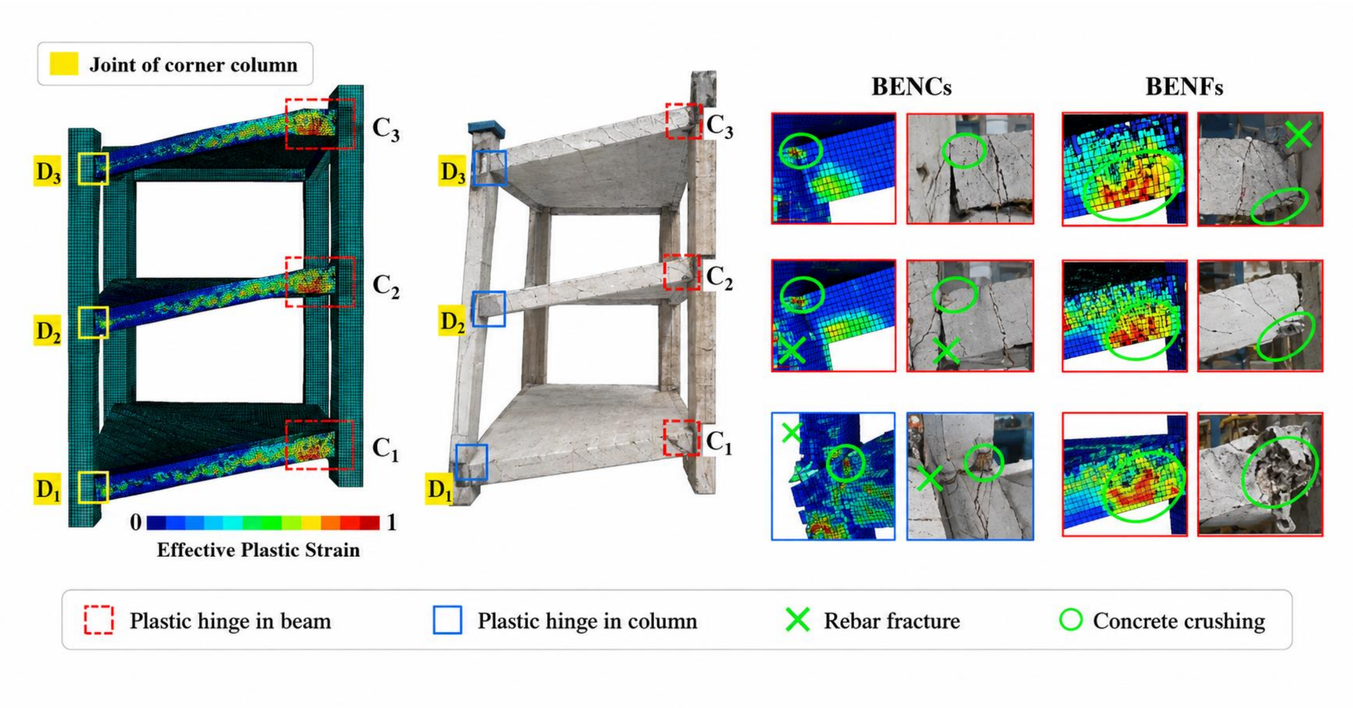

(b)

Fig 6. Distribution of plastic hinge locations obtained from numerical simulations and experimental observations for (a) Specimen S1 and (b) Specimen S3 (shown for the side beam CD facade)

Please cite this article as: Beiranvand, P., Lari, F., Alipour, M., and Maleki, M. (2026). Effect of storey number on Vierendeel mechanism in progressive collapse of RC frame structures. *Journal of Civil Engineering and Structures*, 10(1), pp. 17-23.

3. Influence of storey number on Vierendeel mechanism

To systematically examine the role of the number of stores in activating the Vierendeel mechanism, a series of numerical substructure models were developed, ranging from one to six storeys. These models, designated S1 through S6 (where the numeral indicates the total number of storeys), were all derived from the validated FE modelling strategy described in Section 2. The comparative assessment focused on two primary aspects: (i) the evolution and spatial distribution of plastic hinges, and (ii) the characteristic load–displacement responses. Given that the post-peak branches of all curves exhibited a steady descending trend after reaching the maximum load, the simulations were terminated at a vertical displacement of 300 mm, as this range was deemed sufficient to capture the governing mechanisms without incurring unnecessary computational expense.

3.1. Plastic hinge development patterns

Fig. 7 illustrates the plastic hinge distributions observed across all substructure configurations. For the single-storey specimen (S1), the primary energy-dissipating zones were confined to the beam ends adjacent to the fixed column supports (identified as BENF locations) and a single yield line that developed within the slab panel. This pattern is characteristic of a pure cantilever flexural response, with no evidence of load redistribution through upper levels.

In stark contrast, the multi-storey assemblies (S2 through S6) exhibited a markedly more complex hinge pattern. In these models, plastic hinges consistently formed at the beam ends near the fixed columns (BENF) across every storey level. Additionally, however, hinges appeared at the beam ends near the corner column (BENC) in all storeys above the ground floor i.e., from the second storey upwards. A further distinctive feature was the formation of a plastic hinge at the lower extremity of the corner column within the first storey. This hinge, which was absent in the single-storey case, indicates a shift in the load-transfer mechanism: the corner column in the lowest storey is subjected to significant bending demands, thereby contributing to the overall resistance through a column-bending mode. Moreover, yield lines were observed on every slab of the multi-storey models, confirming that the floor system also participates in the global response.

In summary, the transition from a single-storey to a multi-storey system introduces two additional categories of plastic hinges: (a) beam hinges at the inner face of the corner column in the upper storeys, and (b) a column hinge at the base of the corner column in the first storey. These additional hinges are the direct manifestation of the Vierendeel mechanism, as they enable the transfer of shear and bending moments through the frame without diagonal bracing.

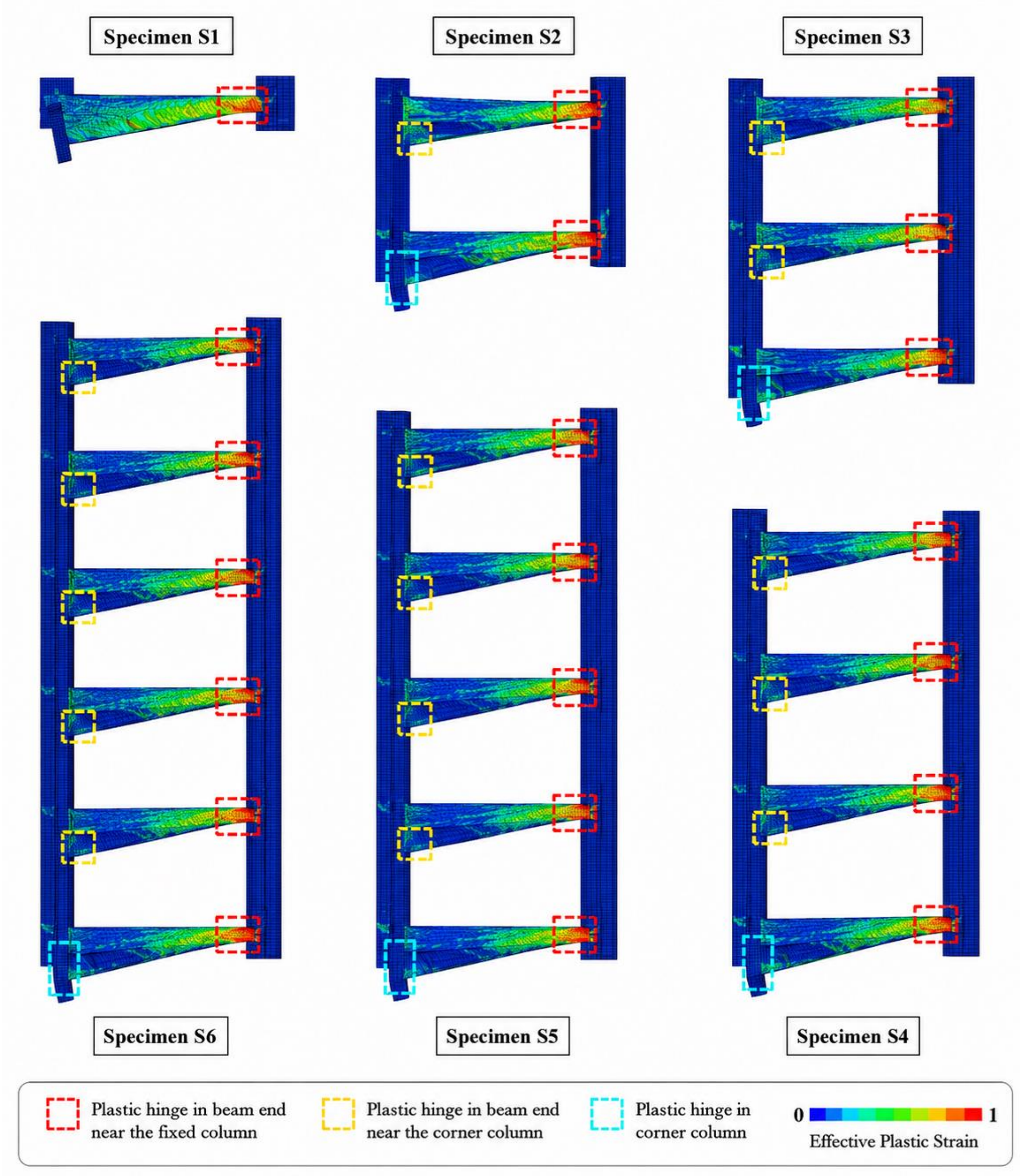

Fig 7. Development of plastic hinges in all substructure models with storey numbers ranging from one to six.

Please cite this article as: Beiranvand, P., Lari, F., Alipour, M., and Maleki, M. (2026). Effect of storey number on Vierendeel mechanism in progressive collapse of RC frame structures. *Journal of Civil Engineering and Structures*, 10(1), pp. 17-23.

3.2. Load–Vertical displacement behaviour

To enable a meaningful comparison between substructures with different total heights, the applied load was normalized by the number of storeys, yielding an average storey load. Fig. 8 presents the average load versus vertical displacement curves for all six specimens, while Table 2 summarizes the key response parameters namely, the ultimate average resistance and the corresponding displacement at peak load.

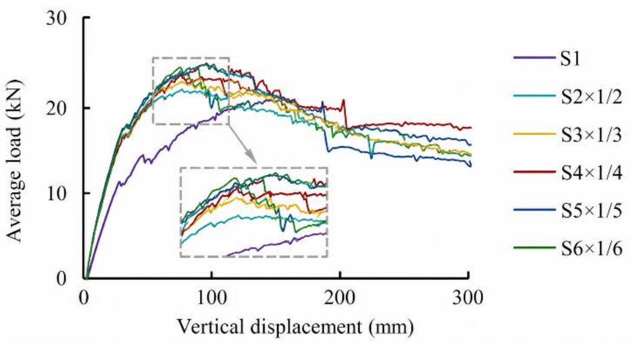

Fig 8. Average load–vertical displacement curves (load per storey) for specimens with different numbers of storeys.

The average ultimate resistances recorded for Specimens S1 through S6 were 20.1 kN, 24.6 kN, 24.0 kN, 23.9 kN, 23.7 kN, and 23.4 kN, respectively. These values clearly demonstrate that the multi-storey substructures consistently outperform the single-storey reference, with improvements ranging from approximately 14.1 % to 18.3 %. This enhancement is directly attributable to the activation of the Vierendeel mechanism, which mobilizes additional load-carrying capacity from the upper storeys and the lower portion of the corner column.

However, a closer inspection of the data reveals a subtle but discernible trend: as the number of storeys increases beyond two, the average ultimate resistance exhibits a slight but progressive decline. The peak value occurs for the two-storey model (S2), after which the resistance reduces gradually, with the six-storey model (S6) showing the lowest average ultimate load among the multi-storey group. This reduction can be explained by the fact that the plastic hinge at the base of the first-storey corner column which is a major source of VM-related resistance provides a greater contribution than the beam hinges at the BENC locations in the upper storeys. In taller frames, the relative efficiency of each additional storey diminishes because the upper-level beam hinges are less effective in transmitting loads to the foundation.

In terms of deformation capacity, the displacements corresponding to the ultimate resistance were 148 mm, 96 mm, 91 mm, 76 mm, 76 mm, and 76 mm for S1 through S6, respectively. The single-storey system exhibited the largest deformation at peak load, consistent with its cantilever-like behaviour, which allows substantial rotation at the beam ends. Conversely, the multi-storey frames displayed markedly smaller displacements, as their beams deformed in double-curvature due to the restraining effect of the upper storeys and the column hinge. This double-curvature action not only increases the initial stiffness but also reduces the ductility demand at the ultimate state. Notably, the displacement at peak load stabilized at approximately 76 mm for specimens with four or more storeys, suggesting that beyond a certain height, the deformation characteristics become largely insensitive to further increases in the number of storeys.

Overall, the findings indicate that while the presence of additional storeys significantly enhances the progressive collapse resistance through the Vierendeel mechanism, the marginal benefit per storey tends to decrease with increasing building height. This insight has important implications for the design of tall RC frames, where the contribution of upper storeys to the ALP response should be carefully quantified rather than conservatively neglected.

Table 2. Ultimate resistance and corresponding vertical displacement of substructure models with varying storey numbers.

Specimen	Number of storeys	Ultimate resistance (kN)	Displacement at ultimate resistance (mm)
S1	1	20.1	148
S2	2	49.2	96
S3	3	72.0	91
S4	4	95.6	76
S5	5	118.5	76
S6	6	140.4	76

4. Conclusions

This study systematically investigated the influence of the number of storeys on the activation and quantitative contribution of the Vierendeel mechanism (VM) in reinforced concrete frame structures subjected to progressive collapse following the removal of a corner column. Through validated finite element modelling, a series of substructures ranging from one to six storeys were analyzed with respect to their plastic hinge development, load–displacement behaviour, and resistance mechanisms. The following conclusions are drawn from the findings:

Multi-storey substructures exhibit a fundamentally different plastic hinge pattern compared to their single-storey counterparts. While the single-storey system relied exclusively on beam end hinges adjacent to the fixed supports and a single slab yield line characteristic of a cantilever flexural mechanism the multi-storey frames developed a more distributed yielding pattern. Additional plastic hinges emerged at the beam ends near the corner column in all storeys above the ground level, alongside a distinctive hinge at the lower end of the corner column within the first storey. This redistribution of plasticity is the hallmark of the Vierendeel mechanism, which enables the upper storeys to participate actively in resisting the applied loads.

The Vierendeel mechanism significantly enhances the collapse resistance of multi-storey frames. Normalizing the total resistance by the number of storeys revealed that the average ultimate resistance of multi-storey substructures exceeded that of the single-storey reference by 14.1 % to 18.3 %. This improvement is directly attributable to the additional load-transfer paths created through the column hinge at the base of the corner column and the beam hinges in the upper levels. These mechanisms collectively distribute the imposed loads more evenly throughout the structure, thereby increasing the overall robustness.

The marginal benefit of each additional storey diminishes as the building height increases. Although the presence of upper storeys consistently improved the average resistance, the highest average ultimate load was recorded for the two-storey model (24.6 kN), after which a gradual decline was observed, reaching 23.4 kN for the six-storey configuration. This trend suggests that the first upper storey provides the most substantial contribution to the Vierendeel mechanism, while the efficiency of successive storeys decreases because the beam hinges at the BENC locations in higher levels are less effective than the column hinge in the ground storey. In practical terms, this implies that for tall buildings, the VM contribution from storeys beyond the second or third may be relatively modest and could be conservatively neglected in simplified design approaches without significant loss of accuracy.

Multi-storey frames exhibit higher initial stiffness and lower displacement demands at the ultimate state. The displacement corresponding to the peak resistance decreased markedly from 148 mm in the single-storey model to approximately 76 mm in frames with four or more storeys. This reduction is attributed to the double-curvature deformation pattern imposed on the beams of multi-storey substructures, which restricts rotational freedom and enhances the system's overall rigidity. The stabilization of this displacement value beyond four storeys indicates that a threshold height exists beyond which further increases in the number of levels do not significantly affect the deformation capacity at failure.

Practical implications for progressive collapse design. The findings underscore the importance of explicitly accounting for the Vierendeel mechanism when assessing the alternate load path (ALP) resistance of multi-storey RC frames particularly in low- to mid-rise buildings where the VM contribution is most pronounced. Current design practice, which often relies on single-storey substructure tests, may underestimate the actual collapse resistance of taller frames by neglecting the beneficial effects of the upper storeys. Conversely, for very tall structures, the diminishing marginal benefit of additional storeys suggests that a simplified upper-bound estimate perhaps limiting the VM contribution to the first two or three storeys above the removed column could provide a reasonable and conservative design approximation.

Recommendations for future research. While this study focused on regular frame configurations with identical storey heights and reinforcement detailing, further investigations are warranted to examine the influence of irregular layouts, varying span lengths, and different column removal scenarios (e.g., interior or edge columns). Additionally, the dynamic effects associated with sudden column loss which were not considered in this quasi-static analysis may alter the activation sequence of plastic hinges and the relative contribution of the Vierendeel mechanism. Experimental validation using full-scale multi-storey tests would also be valuable to corroborate the numerical trends observed in this study.

In conclusion, the present research demonstrates that the number of storeys is a critical parameter governing the development of the Vierendeel mechanism in RC frames under corner column removal. The activation of additional plastic hinges in the upper storeys and at the base of the corner column provides a meaningful increase in collapse resistance, although this benefit is not linearly proportional to the building height. These insights contribute to a more refined understanding of progressive collapse mechanisms and offer a basis for improving current design guidelines.

Conflict of interest

There is not conflict of interest.

References

[1] Adam, J. M., Buitrago, M., Bertolesi, E., Sagaseta, J., & Moragues, J. J. (2020). Dynamic performance of a realscale reinforced concrete building test under a cornercolumn failure scenario. *Engineering Structures*, 210, 110414.

https://doi.org/10.1016/j.engstruct.2020.110414

[2] Buitrago, M., Makound, N., Moragues, J. J., Sagaseta, J., & Adam, J. M. (2023). Robustness of a fullscale precast building structure subjected to cornercolumn failure. *Structures*, 52, 824–841.

https://doi.org/10.1016/j.istruc.2023.04.006

[3] Department of Defense. (2009). Unified Facilities Criteria (UFC): Design of buildings to resist progressive collapse (UFC 402303). U.S. Department of Defense.

[4] Du, K., Bai, J., Teng, N., Yan, D., & Sun, J. (2020). Experimental investigation of asymmetrical reinforced concrete spatial frame substructures against progressive collapse under different column removal scenarios. *The Structural Design of Tall and Special Buildings*, 29, e1717.

https://doi.org/10.1002/tal.1717

[5] European Committee for Standardization. (2006). Eurocode 1: Actions on structures – Part 17: General actions – Accidental actions (EN 199117). CEN.

[6] Li, Y., Lu, X., Guan, H., & Ren, P. (2016). Numerical investigation of progressive collapse resistance of reinforced concrete frames subject to column removals from different stories. *Advances in Structural Engineering*, 19(2), 314–326.

https://doi.org/10.1177/1369433215626223

[7] Lim, N. S., Tan, K. H., & Lee, C. K. (2017). Experimental studies of 3D RC substructures under exterior and corner column removal scenarios. *Engineering Structures*, 150, 409–427.

https://doi.org/10.1016/j.engstruct.2017.07.054

[8] Ministry of Housing and UrbanRural Development of China. (2010a). Code for design of concrete structures (GB 500102010). China Architecture & Building Press. (In Chinese)

[9] Ministry of Housing and UrbanRural Development of China. (2010b). Code for seismic design of buildings (GB 500112010). China Architecture & Building Press. (In Chinese)

[10] Qian, K., & Li, B. (2012a). Dynamic performance of RC beamcolumn substructures under the scenario of the loss of a corner column Experimental results. *Engineering Structures*, 42, 154–167.

https://doi.org/10.1016/j.engstruct.2012.04.017

[11] Qian, K., & Li, B. (2012b). Slab effects on response of reinforced concrete substructures after loss of corner column. *ACI Structural Journal*, 109(6), 845–856.

https://doi.org/10.14359/51684176

[12] Qian, K., Cheng, J. F., Weng, Y. H., & Fu, F. (2021). Effect of loading methods on progressive collapse behavior of RC beamslab substructures under corner column removal scenario. *Journal of Building Engineering*, 44, 103258.

https://doi.org/10.1016/j.jobe.2021.103258

[13] Qiao, H., Yang, Y., & Zhang, J. (2018). Progressive collapse analysis of multistory moment frames with varying mechanisms. *Journal of Performance of Constructed Facilities*, 32(4), 04018043.

https://doi.org/10.1061/(ASCE)CF.19435509.0001188

[14] Qiao, H., Luo, C., Wei, J., & Chen, Y. (2020). Progressive collapse analysis for steelbraced frames considering Vierendeel action. *Journal of Performance of Constructed Facilities*, 34(4), 04020069.

https://doi.org/10.1061/(ASCE)CF.19435509.0001464

[15] Qin, W., Xi, Z., Liu, X., Feng, P., Ou, X., & Yang, J. (2022). Experimental and theoretical analyses of the progressive collapse resistance of NSM strengthening RC frames after the failure of a corner column. *Journal of Building Engineering*, 47, 103805.

https://doi.org/10.1016/j.jobe.2021.103805

[16] Sasani, M., Bazan, M., & Sagiroglu, S. (2007). Experimental and analytical progressive collapse evaluation of actual reinforced concrete structure. *ACI Structural Journal*, 104(6), 731–739.

https://doi.org/10.14359/18964

[17] Sasani, M., & Sagiroglu, S. (2008). Progressive collapse resistance of Hotel San Diego. *Journal of Structural Engineering*, 134(3), 478–488.

https://doi.org/10.1061/(ASCE)07339445(2008)134:3(478)

[18] Sasani, M., Kazemi, A., Sagiroglu, S., & Forest, S. (2011). Progressive collapse resistance of an actual 11story structure subjected to severe initial damage. *Journal of Structural Engineering*, 137(9), 893–902.

https://doi.org/10.1061/(ASCE)ST.1943541X.0000471

[19] U.S. General Services Administration. (2003). Progressive collapse analysis and design guidelines for new federal office buildings and major modernization projects. GSA.

[20] Xu, J., Wang, S., Liu, K., Quan, X., & Dong, F. (2021). Study on collapse resistance of RC frame under the corner column removal scenario. *Materials*, 14(23), 7157.

https://doi.org/10.3390/ma14237157

Please cite this article as: Beiranvand, P., Lari, F., Alipour, M., and Maleki, M. (2026). Effect of storey number on Vierendeel mechanism in progressive collapse of RC frame structures. *Journal of Civil Engineering and Structures*, 10(1), pp. 17-23.